

See discussions, stats, and author profiles for this publication at: <https://www.researchgate.net/publication/263709462>

Novel Ferrocenyl-Terminated Linear-Dendritic Amphiphilic Block Copolymers: Synthesis, Redox-Controlled Reversible Self-Assembly, and Oxidation-Controlled Release

ARTICLE *in* LANGMUIR · JULY 2014

Impact Factor: 4.46 · DOI: 10.1021/la501652r · Source: PubMed

CITATION

1

READS

60

6 AUTHORS, INCLUDING:



[Renfeng Dong](#)

South China University of Technology

15 PUBLICATIONS 120 CITATIONS

[SEE PROFILE](#)



[Biye Ren](#)

South China University of Technology

55 PUBLICATIONS 795 CITATIONS

[SEE PROFILE](#)



[Zhen Tong](#)

South China University of Technology

196 PUBLICATIONS 3,674 CITATIONS

[SEE PROFILE](#)

Novel Ferrocenyl-Terminated Linear–Dendritic Amphiphilic Block Copolymers: Synthesis, Redox-Controlled Reversible Self-Assembly, and Oxidation-Controlled Release

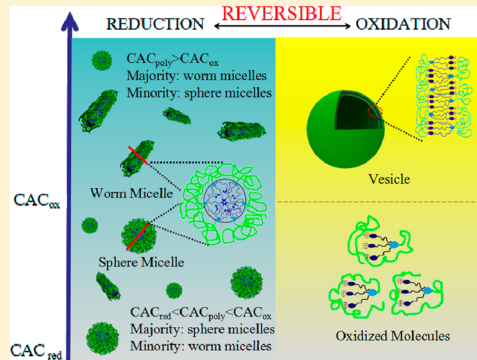
Xueyi Chang,[†] Renfeng Dong,[†] Biye Ren,^{*,†} Zhiyu Cheng,[‡] Jun Peng,[†] and Zhen Tong[†]

[†]Research Institute of Materials Science, South China University of Technology, Guangzhou 510640, People's Republic of China

[‡]College of Chemistry and Environmental Engineering, Dongguan University of Technology, Dongguan 523808, People's Republic of China

S Supporting Information

ABSTRACT: Novel linear–dendritic amphiphilic block copolymers with hydrophilic poly(ethylene glycol) (PEG) block and hydrophobic Percec-type dendrons containing ferrocenyl terminals were synthesized by the esterification reaction of poly(ethylene glycol) methyl ether with ferrocenyl-terminated alkyl-substituted benzoic acid dendrons. On the basis of the results that the critical aggregation concentration (CAC_{ox}) of the oxidation state polymer is much higher than CAC_{red} of the corresponding reduction state, these polymers can reversibly self-assemble into various aggregates, such as spherical, wormlike micelles, and vesicles, and also disassemble into irregular fragments in aqueous solution by redox reaction when changing the polymer concentrations. Copolymer PEG₄₅-*b*-Fc₃ (3) with 3,4,5-tris(11-ferrocenylundecyloxy) benzoic acid (2) can self-assemble into nanoscale wormlike micelles when the polymer concentration in aqueous solution is above its CAC_{ox} . These wormlike micelles can be transformed into nanosized vesicles by Fe₂(SO₄)₃ and regained by vitamin C. Interestingly, copolymer PEG₄₅-*b*-Fc₂ (5) with 3,5-bis(11-ferrocenylundecyloxy) benzoic acid (4) can reversibly self-assemble into spherical micelles with two different sizes by redox reaction above the CAC_{ox} indicating that the terminal hydrophobic tail number of dendrons plays a key role in determining the self-assembled structures. Furthermore, rhodamine 6G (R6G)-loaded polymer aggregates have been successfully used for the oxidation-controlled release of loaded molecules, and the release rate can be mediated by the concentrations of oxidant and copolymers. The results provide an effective approach to the reversible self-assembly of linear–dendritic amphiphilic block copolymers and also promise the potential of these novel redox-responsive amphiphilic block copolymers in drug delivery systems, catalyst supports, and other research fields.



INTRODUCTION

The macromolecular self-assembly based on specific non-covalent interactions underwent rapid development in the past 30 years due to the appearance of many new concepts, principles, and methods.^{1–3} Various topological structural polymers (block copolymers, star polymers, hyperbranched polymers, linear–dendritic copolymers, and dendrimers, etc.), small amphiphilic molecules, micronanoparticles (gold nanoparticles, carbon nanotubes, fullerenes, graphene, and nanocapsules, etc.) are the most-used building blocks for the construction of complex nanostructures with multiscales, multicomponents, and multifunctions.^{2–7} Furthermore, the ways to regulate the self-assembled structures and functions have also been established and developed by means of the solvent polarity,^{8,9} redox switches,^{10–15} temperature,^{16–19} photochemistry,^{20–24} pH,^{25–27} electrochemistry,^{28–30} host–guest modulation,³¹ and specific enzyme recognition.³² For example, Jiang et al. designed an optical switching vesicle by the photochemical properties of azobenzene and host–guest assembly.³³ Recently, macromolecular controlled self-assembly

has been used to prepare nanosized micelles, vesicles, lamella, tubes, spheres, spirals, and more ordered and complex micronanostructures,^{34–39} even functional materials and devices with a photoelectric response, catalysis, drug release, testing, and biomedical applications, which greatly promoted the development of materials, life, and information sciences and related fields.^{2–4,40–42} For example, Oriol et al. reported a light-induced release system based on the photoresponsive reversible self-assembly and disassembly of amphiphilic linear–dendritic block copolymers with a poly(ethylene glycol) (PEG) block and dendrons containing different percentages of hydrocarbon chains (C18) and 4-isobutoxy zobenzene (AZO).⁴³

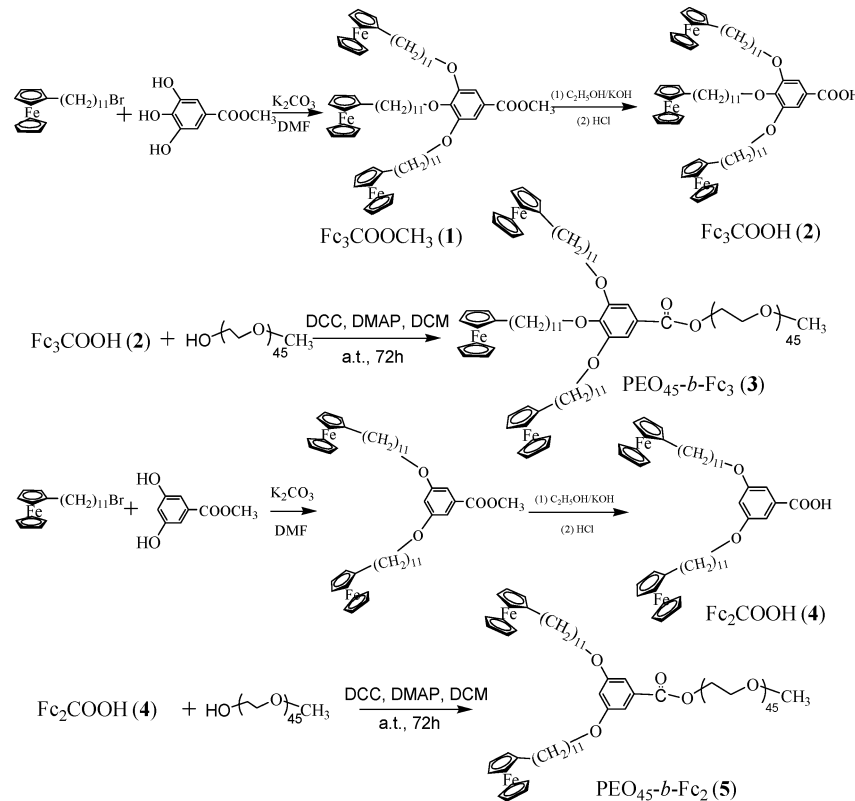
On the other hand, redox-responsive polymers have recently gained considerable attention due to their potential in controllable delivery and release in physiological environments, where redox reactions are widely and constantly present.^{10,12} As

Received: April 29, 2014

Revised: July 5, 2014

Published: July 6, 2014



Scheme 1. Synthesis Routes of Ferrocenyl-Terminated Linear–Dendritic Amphiphilic Block Copolymers

we know, redox-responsive polymers mainly contain sulfur,^{15,44} selenium,^{10,12} viologen,¹⁴ ferrocene,^{11,28,29} and other functional groups. Some research has been focused on the controlled self-assembly and disassembly of redox-responsive polymers. For example, side-chain selenium-containing amphiphilic poly(ethylene oxide-*b*-acrylic acid) block copolymers PEO-*b*-PAA-Se can form spherical micelles. The selenide group can change to hydrophilic selenoxide by hydrogen peroxide, leading to the disassembly of spherical micelles; selenoxide can be reduced to selenide by vitamin C, thus recovering the spherical aggregates.¹⁰ Napoli et al. reported oxidation-responsive vesicles from amphiphilic block copolymers of ethylene glycol and propylene sulfide.⁴⁴ Compared to sulfur and selenium, hydrophobic ferrocene groups can be quickly oxidized to yield hydrophilic ferrocenium cations and then reversibly recovered by reducing agents by chemical and electrochemical means, which results in a reversible change in hydrophilicity without a change in molecular structure because only the gain and loss of electrons occur in the redox process of ferrocenyl groups, which is a great advantage to the construction of reversible self-assembly and disassembly by means of changing molecular structures.^{11,28,45–48} For example, polystyrene-*b*-polyferrocenylsilane (PS-*b*-PFS) can form spherical micelles after adding oxidant in dichloromethane and disassemble by a reducing agent.⁴⁶ Side-chain ferrocene-containing amphiphilic block copolymers conjugated with aminoxy model drug *O*-benzylhydroxylamine can form spherical micelles, and the size of the micelles presents a reversible redox-triggered transition.¹¹ Moreover, ferrocene can exactly form a 1:1 inclusion complex with β -cyclodextrin (β -CD), and the charged species (Fc^+) can dissociate rapidly from the cavity of β -CD, which can be used to construct supramolecular systems with redox-controlled reversible self-assembly.^{28,29} Thus, it is of particular interest how to

take advantage of ferrocene groups to develop novel redox-controlled reversible self-assembly systems. For this purpose, we attempted to introduce Percec-type dendrons containing ferrocenyl-terminals into PEG block to construct redox-controlled reversible self-assembly systems considering the multicomponent constitutions, multivalent characteristics, and unique self-assembly properties of linear–dendritic amphiphilic block copolymers. As is well known, above the critical aggregation concentration (CAC), polymer amphiphiles can self-assemble into aggregates by hydrophobic association in aqueous solution.^{49,50} For this kind of ferrocene-containing amphiphilic block copolymer, the CAC_{red} of the reduction state polymers would be lower than the CAC_{ox} of the corresponding oxidation state polymers because hydrophobic ferrocene groups can be oxidized to yield hydrophilic ferrocenium cations. Therefore, it is expected that these polymers would reversibly self-assemble into various aggregates when the polymer concentrations in aqueous solution are above their CAC_{ox} . And these polymers would also self-assemble and disassemble by redox reaction when the concentrations of polymers are between their CAC_{red} and CAC_{ox} values. However, little study on the redox-controlled reversible self-assembly and disassembly of linear–dendritic amphiphilic block copolymers without changing their chemical structure has been reported.

In the present study, two novel linear–dendritic amphiphilic block copolymers with a PEG block and Percec-type alkyl substituted benzoic acid dendrons containing ferrocenyl terminals (Scheme 1) were synthesized by the esterification reaction of poly(ethylene glycol) methyl ether with ferrocenyl-terminated alkyl-substituted benzoic acid dendrons, and their redox-controlled reversible self-assembly and disassembly behavior in aqueous solution was investigated by transmission electron microscopy (TEM) and dynamic light scattering

(DLS). The main goal of this study is to establish a suitable method of regulating the redox-controlled reversible self-assembly and disassembly behavior of these polymers in aqueous solution by reversible chemical or electrochemical reactions without changing their molecular structure. The second goal is to demonstrate the potential of these redox-controlled reversible self-assembly and disassembly systems in drug delivery systems, catalyst supports, and other research fields by using rhodamine 6G (R6G)-loaded polymer aggregates for the oxidation-controlled release of loaded molecules.

EXPERIMENTAL SECTION

Materials. Poly(ethylene glycol) methyl ether (Flakes, average $M_n = 2000$), methyl 3,4,5-trihydroxybenzoate (Aldrich, purity 98%), methyl 3,5-dihydroxybenzoate (Aldrich, purity 97%), 4-dimethylaminopyridine (DMPEP) (Shanghai Medpep, purity 99%), and *N,N'*-dicyclohexylcarbodiimide (DCC) (Aladdin, purity 99%) were used as received. 11-Bromoundecyl ferrocene was synthesized according to our previous report.⁵¹ Dichloromethane (CH_2Cl_2) was dried with CaH_2 and distilled under normal pressure prior to use. All of the other chemicals were analytical reagents and purified according to the standard procedures. Water used in all experiments was deionized and filtered with a Millipore purification apparatus with a resistivity of more than $18.0 \text{ M}\Omega\cdot\text{cm}$.

Instruments. The ^1H NMR spectra were recorded on a Bruker Avance 400 (300 MHz) spectrometer. The carbon and hydrogen contents (wt %) were determined with a Vario EL elemental analyzer. The size distribution of the aggregates was analyzed at 25 °C by dynamic light scattering (DLS), a Malvern Nano-ZS 90 Zetasizer using a monochromatic coherent He–Ne laser (633 nm) as the light source, and a detector that detected the scattered light at an angle of 90°. Molecular weights and molecular weight distributions of polymers were measured by gel permeation chromatography (GPC) with a Waters 515 pump/M717 data module/R410 differential refractometer using THF as the mobile phase with a flow rate of 1.5 mL/min, distributed polystyrene as a standard, and a column temperature of 40 °C. UV-vis absorption spectra were determined on a Hitachi U-3010 UV-vis spectrophotometer. Transmission electron microscopy (TEM) images were obtained from a JEM-2100HR microscope with an acceleration voltage of 200 kV, and samples were taken through the homemade atomizer to aerospray cellulose-coated copper grids⁵² and then stained with 2 wt % uranyl acetate before observation. Surface tensions were obtained from a surface tension meter (Dataphysics OCA20, Germany) at 25 °C. Fourier transform infrared (FT-IR) spectra were obtained on a Thermo Nicolet 6700 spectrometer using KBr substrates. Cyclic voltammograms (CV) were obtained on a CHI 660C electrochemical workstation (CH Instruments, Shanghai) at room temperature under an argon atmosphere using a three-electrode system. In DMF solution bearing 0.1 M (n-Bu)₄NClO₄, a glassy carbon electrode was used as the working electrode, a platinum electrode was used as the counter electrode, and saturated calomel electrode (SCE) was used as the reference electrode which was connected to test solutions by a salt bridge. In 0.1 M NaCl aqueous solution, platinum plate electrodes (0.2 cm × 1.0 cm) were selected as the working electrode and the counter electrode, respectively, and SCE was selected as the reference electrode.

Synthesis Procedure. The synthesis routes of ferrocene-terminated linear–dendritic amphiphilic block copolymers 3 and 5 are shown in Scheme 1. 3,4,5-Tris(11-ferrocenylundecyloxy) benzoic acid (2) and 3,5-bis(11-ferrocenylundecyloxy) benzoic acid (4) were synthesized according to the same procedure reported in our previous study in detail.⁵³ The synthesis of copolymer 3 (PEG₄₅-b-Fc₃) is taken as an example. First, to a 100 mL round-bottomed flask with a magnetic stirrer, a mixture of 0.3 g (0.253 mmol) of 2 and 0.615 g (0.307 mmol) of PEG2000-OCH₃ in 15 mL of dry CH_2Cl_2 were added. DMAP (75 mg, 0.614 mmol) and DCC (70 mg, 0.339 mmol) in 10 mL of dry CH_2Cl_2 were slowly added to the flask. The mixture

was stirred at 25 °C. After about 72 h, the reaction endpoint was determined by thin layer chromatography (TLC) analysis. Subsequently, the catalyst was removed by filtration, and the solvent was removed in vacuo. The crude product was then purified by silica gel column chromatography (eluent $\text{CH}_2\text{Cl}_2/\text{CH}_3\text{OH} = 8:1$ by volume, $R_f = 0.67$) to yield 0.37 g (46 wt %) of yellow solid polymer 3. ^1H NMR and FT-IR for copolymer 3 are shown in Figure 1 and Figure S11,

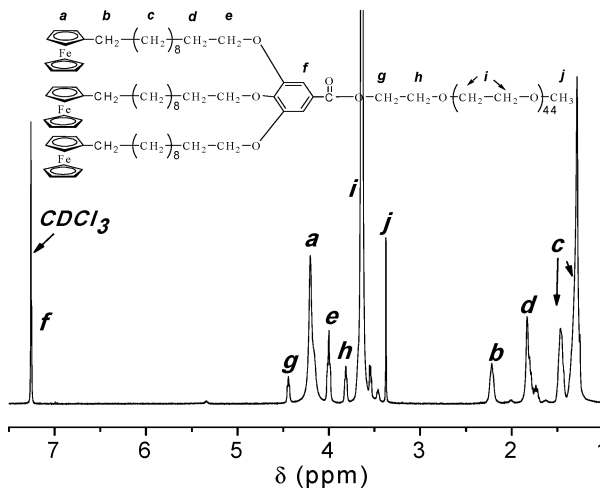


Figure 1. ^1H NMR spectrum of polymer 3 measured in CDCl_3 .

respectively. ^1H NMR (CDCl_3 , TMS) δ (ppm) 7.25 (s, 2H, Ar-H), 4.44 (t, 2H, Ar-COO-CH₂-), 4.20 (m, 27H, H(Cp)), 3.99 (t, 6H, -CH₂-O-Ar), 3.81 (t, 2H, Ar-COO-CH₂-CH₂-), 3.64 (m, 176H, Ar-COO-CH₂-CH₂-O-CH₂-CH₂-), 3.37 (s, 3H, -O-CH₃), 2.21 (t, 6H, Cp-CH₂-), 1.73 (m, 6H, -CH₂-CH₂-O-Ar), 1.46–1.28 (m, 48H, -CH₂-). FT-IR (KBr): 3090, 1468, 1118, 998, and 815 (characteristics of ferrocene group absorption peaks), 1715 (ν_s C=O), 2924 (ν_{as} CH₂), 2856 (ν_s CH₂), 1105 cm^{-1} (ν_s C–O–C). Anal. Calcd for $\text{C}_{161}\text{H}_{278}\text{O}_{50}\text{Fe}_3$: C, 60.78; H, 8.81. Found: C, 60.75; H, 8.84.

Copolymer 5 (PEG₄₅-b-Fc₂) was synthesized according to a similar method to 3, and its yield was 49.2%. FT-IR and ^1H NMR for copolymer 5 are shown in Figures S12 and S13, respectively. ^1H NMR (CDCl_3 , TMS) δ (ppm) 7.16 (d, 2H, Ar-H), 6.62 (t, 1H, Ar-H), 4.44 (t, 2H, Ar-COO-CH₂-), 4.11 (m, 18H, H(Cp)), 3.96 (t, 4H, -CH₂-O-Ar), 3.81 (t, 2H, Ar-COO-CH₂-CH₂-), 3.64 (m, 176H, Ar-COO-CH₂-CH₂-O-CH₂-CH₂-), 3.37 (s, 3H, -O-CH₃), 2.28 (t, 4H, Cp-CH₂-), 1.76 (m, 4H, -CH₂-CH₂-O-Ar), 1.46–1.28 (m, 32H, -CH₂-). FT-IR (KBr): 3092, 1468, 1118, 998, and 815 (characteristics of ferrocene groups absorption peaks), 1720 (ν_s C=O), 2921 (ν_{as} CH₂), 2851 (ν_s CH₂), 1111 cm^{-1} (ν_s C–O–C). Anal. Calcd for $\text{C}_{140}\text{H}_{248}\text{O}_{49}\text{Fe}_2$: C, 59.48; H, 8.84. Found: C, 59.44; H, 8.86.

Preparation of Polymer Aggregates. The linear–dendritic amphiphilic block copolymer (75.0 mg) was dissolved in 1 mL of THF and then added to 10 mL of deionized water dropwise under electromagnetic stirring. The solution was stirred at room temperature in air for 12 h to allow THF to evaporate slowly and then dialyzed for 3 days (cutoff membrane: 2000 g mol⁻¹) to remove the remaining THF. The volume of the solution was increased to 15 mL with the addition of deionized water in order to obtain a 5.0 g L⁻¹ polymer solution for further experiments.

To prepare rhodamine 6G (R6G)-loaded micelles, 70 mg of polymer and 5 mg of R6G were dissolved in 1 mL of *N,N*-dimethylformamide (DMF) and dropped into 10 mL of deionized water and stirred at room temperature for 12 h. The solution was dialyzed for 3 days (cutoff membrane: 2000 g mol⁻¹) to remove the remaining DMF and excess R6G until the water outside the dialysis tube exhibited negligible R6G. The final concentration of polymer was 5.0 g L⁻¹.

Redox Response of Polymer Micelles. The aqueous solution of the linear–dendritic amphiphilic block copolymer (5 mL, 5.0 g L⁻¹)

was treated with 0.52 equiv of $\text{Fe}_2(\text{SO}_4)_3$ corresponding to the total ferrocene units in polymer and stirred several minutes until the yellow color of the micelle dispersion turned blue. To reduce the oxidized polymers, vitamin C (0.55 equiv) was added to the oxidized micelles and stirred several minutes until the yellow color was completely recovered. Figure SI4 shows the oxidation and reduction of polymer 3. The solutions were kept at room temperature for further studies.

RESULTS AND DISCUSSION

Polymer Analysis. The structures of the obtained polymers were verified by ^1H NMR spectroscopy and FT-IR spectra. Figure 1 shows the ^1H NMR spectrum of polymer 3. Apart from the characteristic peaks of the $\text{Fc}(\text{CH}_2)_{11}\text{O}-$ (ferrocene protons a, methylene protons b and e) and PEG (methylene protons i) blocks, the peaks of methyl (j) and methylene (g) derived from the PEG block were distinctly observed. The ^1H NMR peak area ratio of the methylene protons (b) to the methyl protons (j) is 2, which is consistent with the theoretical value based on the molecular formula. Also, the peak area ratio of b to j is 4/3 (Figure SI3), which indicates that 5 was synthesized successfully. As shown in the FT-IR spectrum of 3 (Figure SI1), the strong characteristic absorption bands appear at 1715 and 1105 cm^{-1} corresponding to the stretching vibration of the ester group, which also confirms that 3 is successfully synthesized. Because of the induced effect of different substituents, the characteristic absorption bands of the ester group of 5 appear at 1720 and 1115 cm^{-1} , which slightly shifts toward high frequency (Figure SI2). GPC experiments show that the theoretical number-average molecular weights of polymers 3 and 5 (3200 and 2800, respectively) derived from the molecular formula are consistent with the values from GPC measurements (3300 and 3000, respectively), and the molecular weight distributions of polymer 3 and 5 are 1.1 and 1.2, respectively (Table SI1).

Redox Activity of Polymers in Solution. As previously described, the ferrocene groups can be transformed to the ferrocenium salt and undergo reversible redox reactions through chemical and electrochemical means.^{11,28} In order to confirm the electrochemical redox activity of these ferrocene-containing linear-dendritic amphiphilic block copolymers, their electrochemical behavior was studied by CV. The CV results show that both 3 and 5 have reversible redox activity in DMF solution (Figure 2A). Potential differences ΔE ($= E_{\text{pa}} - E_{\text{pc}}$) for the two copolymers are both 81 mV at a scan rate of 100 mV/s. The oxidation peak potential (E_{pa}) and reduction peak potential (E_{pc}) are basically unchanged at the potential scan rate ranging from 50 to 500 mV/s, and there is a good linear relationship between the oxidation peak current and the square root of the potential scan rate for both 3 and 5 (Figure SIS). Thus, these linear-dendritic amphiphilic block copolymers have good electrochemical redox reversibility in DMF solution.

It is noted that the oxidation peak potential became broad and smooth in aqueous solution of polymers and the reduction peak potential migrated to -0.26 and -0.23 V, respectively (Figure 2B). When the polymer solutions were electrochemically oxidized under oxidative potential conditions ($+0.5$ V), the oxidation currents are only about $2 \mu\text{A}$, and they may require several hundreds of hours until the polymers are completely oxidized. Thus, in aqueous solution, the polymer aggregates are difficult to redox control by electrochemical methods rapidly. The reason may be that ferrocenyl groups of polymers are located in the hydrophobic core of micelles in

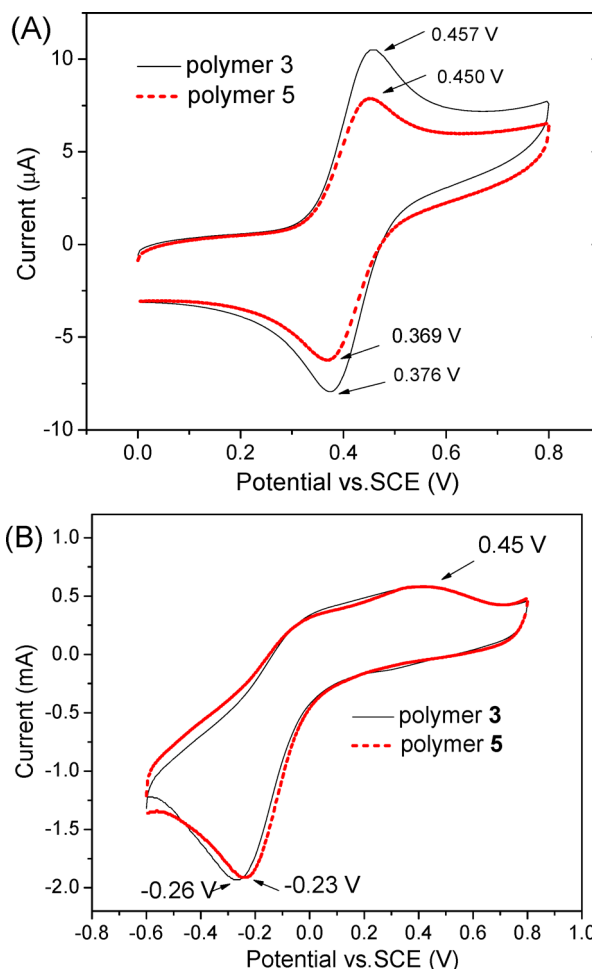


Figure 2. Cyclic voltammograms for 0.5 mM polymers (A) in 0.1 M $(n\text{-Bu})_4\text{NClO}_4$ DMF solution and (B) in 0.1 M NaCl aqueous solution at room temperature at a scan rate of 0.1 V/s.

aqueous solution, which are very difficult to transfer to the electrode surface for electrochemical oxidation. However, as reported by other authors,^{11,45} small molecular oxidants and reducing agents can be spread to the micellar interior by diffusion. Therefore, water-soluble oxidants $\text{Fe}_2(\text{SO}_4)_3$ and reducing agent vitamin C were selected to rapidly attain the reversible redox reactions of these polymeric solutions. The redox status of ferrocene groups can be observed through UV-vis absorption spectra as well; therefore, the polymer redox reaction process was traced using a UV-vis spectrophotometer.⁴⁵ As expected, these ferrocene-containing block copolymers can be rapidly oxidized by adding oxidants and reduced by adding a reducing agent. Figure SI6A shows the UV-vis spectra of 3 before and after oxidation with $\text{Fe}_2(\text{SO}_4)_3$. After a small excess of oxidant $\text{Fe}_2(\text{SO}_4)_3$ was added, the absorption peak at 436 nm of ferrocene groups (in reduced form) disappeared and a new absorption peak at 627 nm appeared, indicating that the ferrocene units in 3 can be oxidized to ferrocenium. The absorption peak of the ferrocene units (in reduced form) was regained and the absorption peak at 627 nm disappeared after adding a small excess of reducing agent vitamin C, indicating that the redox reactions of polymer 3 are reversible. 5 showed the same characteristics as 3 (Figure SI6B). Therefore, the redox-controlled self-assembly behavior of these polymers in

aqueous solution will be carried out through adding oxidants and reducing agents in the following discussion.

Critical Aggregation Concentration (CAC) of Polymers in Aqueous Solution. As is well known, above the critical aggregation concentration (CAC), amphiphiles can self-assemble into aggregates by hydrophobic association in aqueous solution.^{49,50} To study their self-assembly behavior, the CAC values of the linear–dendritic amphiphilic block copolymers were measured by the surface tension method. As shown in Figure 3A, the CACs are about 0.03 and 2.0 g L⁻¹ for

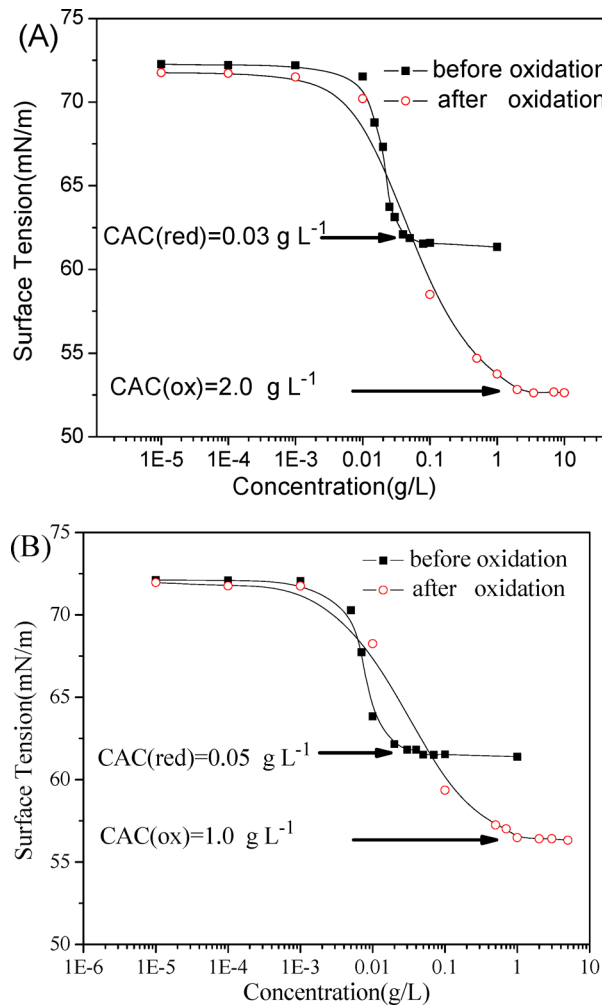


Figure 3. Plots of surface tension against the concentration of polymers 3 (A) and 5 (B) before and after oxidation.

polymer 3 in the reduction and oxidation states, respectively, indicating that the CAC_{ox} of polymer 3 in the oxidation state is much higher than its CAC_{red} in the corresponding reduction state due to the slightly enhanced hydrophilicity of ferrocenium cations, which is consistent with ferrocenyl surfactants.⁴⁹ Similar results are observed for the aqueous solution of 5. The CAC_{red} and CAC_{ox} values are about 0.05 and 1.0 g L⁻¹ for polymer 5, respectively (Figure 3B), indicating that polymer 5 with a two-tailed dendritic hydrophobic block has lower CAC values due to its slightly enhanced hydrophilicity compared to that of 3 with a three-tailed dendritic hydrophobic block. The results suggest that these amphiphilic block copolymers could aggregate and disaggregate by redox reaction when the concentrations of polymers are between their CAC_{red} and

CAC_{ox} values. Furthermore, these polymers should respectively self-assemble into two different aggregates in aqueous solution by redox reaction when the concentrations of polymers are above their CAC_{ox} values. This means that a redox-controlled reversible self-assembly process may be established by the redox reaction of ferrocenyl groups only if the concentrations of polymers are above their CAC_{red} values.

Redox-Controlled Reversible Self-Assemble of Polymers. In order to verify the above considerations, the redox-controlled reversible self-assembly behavior of these ferrocene-containing linear–dendritic amphiphilic block copolymers in aqueous solution was investigated by TEM and DLS. For polymer 3 in an aqueous solution of 0.1 g L⁻¹, which is between its CAC_{red} (0.03 g L⁻¹) and CAC_{ox} (2.0 g L⁻¹), a coexistence of spherical and wormlike micelles with dominantly spherical micelles was observed (Figure 4a). As expected, the aggregates

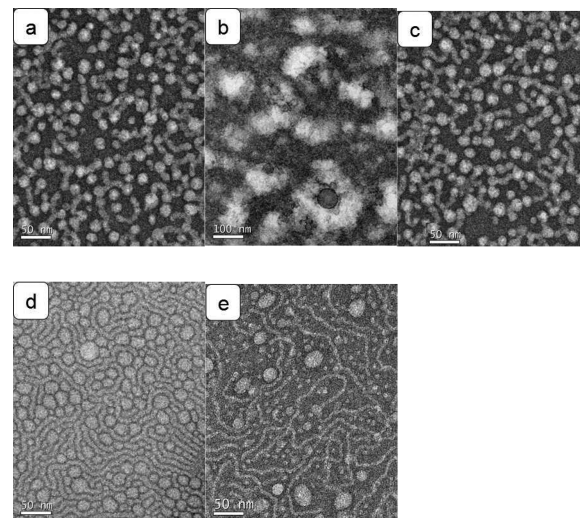


Figure 4. TEM images of polymer 3 micelles (a) and irregular fragments (b) oxidized by Fe₂(SO₄)₃ and (c) reduced by vitamin C in 1.0 g L⁻¹ aqueous solutions. TEM images of polymer 3 micelles in 3.0 g L⁻¹ (d) and 5.0 g L⁻¹ (e) aqueous solutions.

were totally disassembled into discontinuous fragments after oxidation (Figure 4b) and reversibly recovered under reduction by vitamin C (Figure 4c). Interestingly, by increasing the concentrations of polymer 3 from 0.1 to 3.0 g L⁻¹, which is above its CAC_{ox}, the number of spherical micelles gradually decreased, while the number and length of wormlike micelles gradually increased (Figure 4d). Figure 4e clearly shows that wormlike micelles are dominant in an aqueous solution of 5.0 g L⁻¹ polymer 3 besides a small quantity of coexisting spherical micelles. The size of the spherical micelles is about 20–30 nm in diameter, and the size of the wormlike micelles is several hundred nanometers in length and 8 nm in width. In particular, the polymer aggregates turn into vesicles of 40–100 nm diameter after oxidation by Fe₂(SO₄)₃ as observed from Figure 5a, and the wormlike micelles were reversibly recovered under reduction by vitamin C (Figure 5b). It is worth noting that the aggregates of wormlike micelles and vesicles could be repeatedly obtained by redox reaction because this redox process could be cycled at least three times (Figures 5 and 6A), indicating that the redox-controlled reversible self-assembly of polymer 3 was successfully achieved in aqueous solution by redox reaction. The size distributions of the polymer aggregates determined by TEM are further verified by DLS. Figure 6

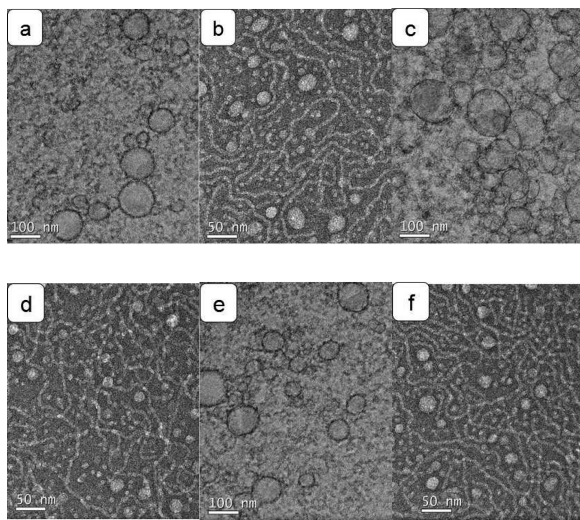


Figure 5. TEM images of polymer 3: aggregates after oxidation (a) by $\text{Fe}_2(\text{SO}_4)_3$ and reduction (b) by vitamin C; the second oxidation (c)–reduction (d) cycle and the third oxidation (e)–reduction (f) cycle. The concentration of the polymeric aqueous solutions is 5.0 g L^{-1} .

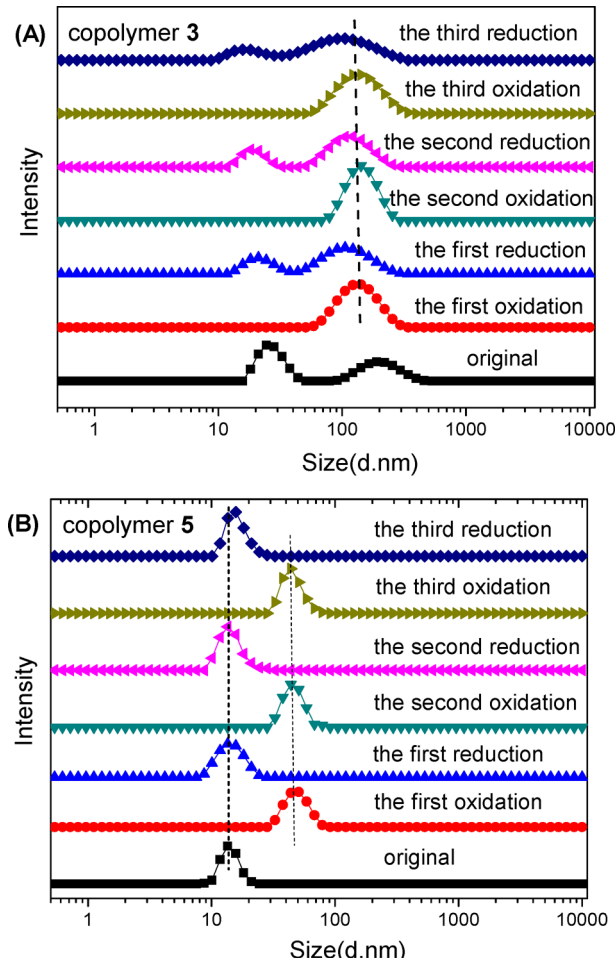


Figure 6. Size distribution of polymer 3 micelles (A) and 5 (B) by DLS in 5 g L^{-1} aqueous solutions for three oxidation–reduction cycles.

shows that diameters of block copolymer micelles determined by DLS are typically larger than those determined by TEM. For instance, the vesicles determined by DLS are 120–140 nm in

diameter for polymer 3 (Figure 6A), which is larger than the 40–100 nm found by TEM (Figure 5a). The reason is that the size distribution of the polymer aggregates determined by DLS reflects the dimensions of both the swollen core and the stretched shell, but the size determined by TEM reflects only conformations in the dry state.¹¹

As for polymer 5 with a two-tailed dendritic hydrophobic block, only spherical aggregates were observed when its concentration was in the range of CAC_{red} to CAC_{ox} (Figure 7a). Analogously, the aggregates were totally disassembled after

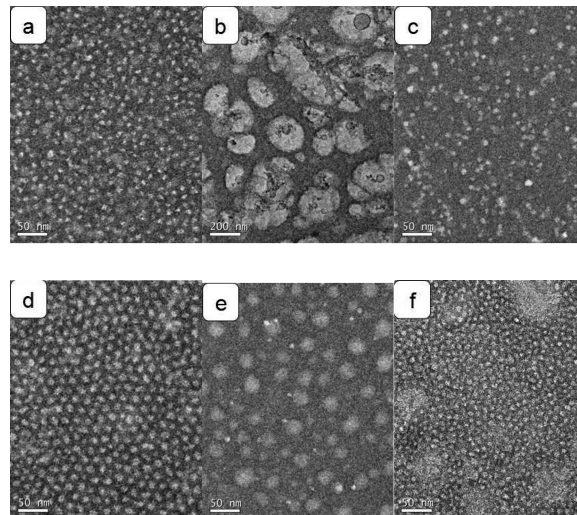


Figure 7. TEM images of polymer 5 micelles (a) and irregular fragments (b) oxidized by $\text{Fe}_2(\text{SO}_4)_3$ and (c) reduced by vitamin C in 0.5 g L^{-1} aqueous solutions. TEM images of polymer 5 micelles (d) and aggregates after oxidation (e) by $\text{Fe}_2(\text{SO}_4)_3$ and reduction (f) by vitamin C in 5 g L^{-1} aqueous solutions.

oxidation, formed discontinuous fragments (Figure 7b), and reversibly recovered under reduction by vitamin C (Figure 7c). When the concentration of 5 increased over its CAC_{ox} , only spherical micelles were observed by TEM, which could also be repeatedly obtained by redox reaction (Figure 6B). The size of spherical micelles determined by TEM is about 8 nm in diameter in an aqueous solution of 5.0 g L^{-1} polymer 5 (Figure 7d), which is smaller than the size distributions (13 nm) of the self-assembly aggregates determined by DLS (Figure 6B). Interestingly, the size of the aggregates increased to about 20–30 nm in diameter after oxidation by $\text{Fe}_2(\text{SO}_4)_3$ (Figure 7e), which is smaller than the size distributions (38 nm) of the self-assembly aggregates determined by DLS (Figure 6B). The larger aggregates of polymer 5 after oxidation by $\text{Fe}_2(\text{SO}_4)_3$ should be attributed to the slightly enhanced hydrophilicity of ferrocenium salt. Furthermore, the large spherical micelles of the oxidation state polymers can be reversibly recovered under reduction by vitamin C (Figure 7f). These results indicate that the redox-controlled reversible self-assembly of polymer 5 can be successfully achieved in aqueous solution by redox reaction.

In order to understand the formation mechanism of redox-controlled reversible aggregation and disaggregation, the self-assembly process of polymer 3 in aqueous solution through microphase separation and geometry selection is given in Figure 8. The length of the extended dendritic hydrophobic block is about 2 nm, and the length of the extended linear hydrophilic block is about 17 nm. Moreover, the width of the wormlike micelle is about 8 nm as observed in Figure 4e.

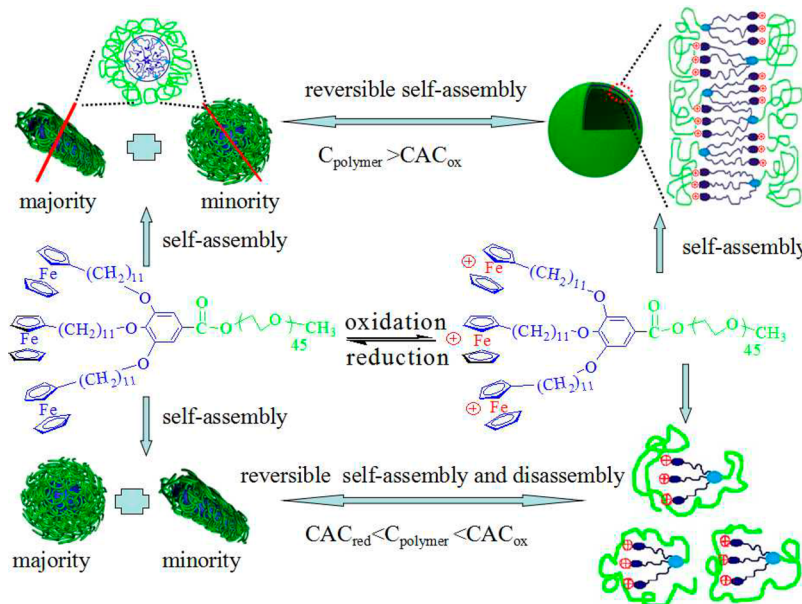


Figure 8. Illustration of the redox-controlled reversible self-assembly for block copolymer $\text{PEG}_{45}\text{-}b\text{-Fc}_3$ (**3**) at different concentrations.

Therefore, the section plane of wormlike micelles should be composed of a hydrophobic core and a hydrophilic shell. The hydrophobic core is composed of several three-tailed dendritic hydrophobic blocks, and the hydrophilic shell is composed of several forniciform hydrophilic blocks, which is consistent with Oriol's and Shen's studies.^{24,43,54} After oxidation by $\text{Fe}_2(\text{SO}_4)_3$, the concentrations of polymer are above the CAC_{ox} , so the self-assembled aggregates were turned into larger vesicles (Figure 5a). This variation in the morphology and size of aggregates is attributed to the oxidation reaction of ferrocene units, which transforms the hydrophobic ferrocene groups to the hydrophilic ferrocenium salt and enhances the hydrophilicity of the dendron block. The thickness of the vesicle wall is about 6 nm in Figure 5a. Thus, the structure of the vesicle wall should be the shape of a two-layered cake, as shown in Figure 8. In addition, when the concentrations of polymers are in the range of CAC_{red} to CAC_{ox} , the aggregates will be disassembled into discontinuous fragments after oxidation.

However, one may wonder why only spherical aggregates appear in the solution of polymer **5** (Figure 7a,d). The reason may be that polymer **5** has a smaller hydrophilic/hydrophobic mass fraction ratio (71/29) than **3** (64/36), and thus the volume fraction of hydrophobic segment is relatively smaller for polymer **5** and cannot provide enough hydrophobic association strength to stabilize wormlike micelles. Hence, polymer **5** forms spherical micelles that are only about 8 nm in diameter, which may be more thermodynamically stable in aqueous solution. As the number of hydrophobic dendritic tails decreases,^{24,54} the morphological transition of the polymer self-assembly aggregates from wormlike micelles to spherical micelles is driven by the minimization of the interfacial energy and qualitatively follows the theory of Israelachvili et al.^{55,56} Compared to the oxidation state polymer **3**, the oxidation state polymer **5** forms smaller micelles because of less charge density and hydrophobic change.

From the above results, one can draw one conclusion that the number of ferroceneterminated hydrophobic chain is a significant contributing factor affecting the associative structures and self-assembled behavior of these linear-dendritic

amphiphilic block copolymers with the same PEG blocks due to their great differences in the hydrophilic/hydrophobic ratio and charge density when redox reaction occurs. In particular, these polymers can reversibly self-assemble into various aggregates, such as spherical, wormlike micelles and vesicles and also disassemble into irregular fragments in aqueous solution by redox reaction when changing the polymer concentrations. These results provide an effective approach to the redox-controlled reversible self-assembly of linear-dendritic amphiphilic block copolymer systems without changing their molecular structure.

Oxidation-Controlled Release of R6G from Polymer Micelles.

As previously mentioned, these ferrocenyl-terminated linear-dendritic amphiphilic block copolymers can self-assemble into wormlike or spherical micelles and disassemble after oxidation when the concentrations of polymers are between their CAC_{red} and CAC_{ox} values; they will be turned into larger vesicles or spherical micelles quickly after oxidation when the concentrations of polymers are above their CAC_{ox} . If drug molecules are loaded into the micelles, they will be quickly released when micelles disaggregate after oxidation at lower concentrations; drug molecules also will be compatibilized to large vesicles and will be slowly released after oxidized at higher concentrations (Figure 9A) with the change in aggregates. In order to utilize this advantage, R6G is used as a model drug molecule, and R6G-loaded polymer **3** micelles were prepared to perform oxidation-controlled release experiments. Five milliliters of R6G-loaded polymer **3** micelles with a concentration of $1.0\text{--}5.0 \text{ g L}^{-1}$ was added to dialysis tubing (cutoff membrane 2000 g mol^{-1}) and placed in a beaker with 200 mL of an oxidant solution $\text{Fe}_2(\text{SO}_4)_3$ with a concentration of $0\text{--}1.0 \text{ g L}^{-1}$. UV-vis measurements were conducted for the oxidant solution outside the dialysis tubing. The absorption intensity of R6G at 527 nm in the water was proportional to its concentration (Figure S17), and the absorbance is calculated as the concentration of R6G from the working curve. Thus, the cumulative release of R6G-loaded polymer solution was calculated according to $\omega_i = V_i C_i / V_0 C_0$, where V_i and V_0 refer to the volumes of the oxidant solution outside the dialysis tube

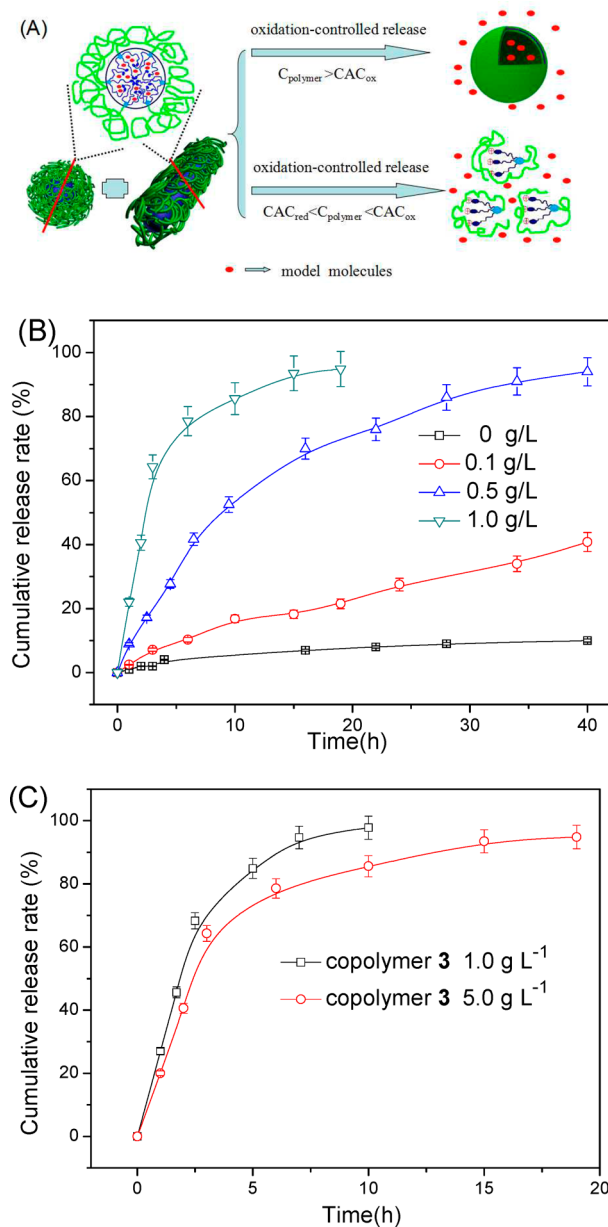


Figure 9. Illustration (A) of the oxidation-controlled release of R6G-loaded polymer 3 solution in different concentrations. Cumulative release (B) of R6G-loaded 5.0 g L⁻¹ polymer 3 solutions after oxidation by different concentrations of oxidant $\text{Fe}_2(\text{SO}_4)_3$. Cumulative release (C) of different concentrations of R6G-loaded polymer 3 solution after oxidation by 1.0 g L⁻¹ oxidant $\text{Fe}_2(\text{SO}_4)_3$.

and R6G-loaded polymer solution, respectively. C_i represents the concentration of R6G in the oxidant solution outside the dialysis tube, and C_0 represents the concentration of R6G in the R6G-loaded polymeric solution, which should be oxidized and diluted before the test.

As shown in Figure 9B, the release of R6G can be mediated by the concentration of oxidant $\text{Fe}_2(\text{SO}_4)_3$. The R6G-loaded polymer solution released less than 10% of R6G after 40 h, indicating that it has good storage properties. About 40% of R6G was released after 40 h in the solution of 0.1 g L⁻¹ $\text{Fe}_2(\text{SO}_4)_3$, but 94% of R6G was released within the same period of time in 0.5 g L⁻¹ $\text{Fe}_2(\text{SO}_4)_3$. With a higher concentration of oxidant such as 1.0 g L⁻¹, R6G was almost completely released after 20 h. This phenomenon should be

caused by the different diffusion rates of oxidants and R6G within different concentrations of oxidant solution. Thus, the change of the concentration of oxidant $\text{Fe}_2(\text{SO}_4)_3$ could effectively control the release rate of R6G from the R6G-loaded polymer solution. R6G-loaded polymer 5 micelles process a very similar release behavior to that of R6G-loaded polymer 3 (Figure SI8). In addition, as mentioned, the release rate of R6G sped up when the polymer concentration was below its CAC_{ox} due to the disassembly of polymers in solution after oxidization, as seen from Figure 9C. Thus, the release rate of R6G can be mediated by the concentrations of oxidant and copolymers.

CONCLUSIONS

Novel ferrocenyl-terminated linear-dendritic amphiphilic block copolymers were synthesized, and their redox-controlled self-assembly behavior in aqueous solution was investigated by TEM and DLS. Redox-controlled reversible self-assembly has been successfully carried out for these polymers in aqueous solution by redox reaction when changing the concentrations of polymers. These copolymers can self-assemble into different aggregates and then disassemble by redox reactions when the concentrations of polymers are in the range of CAC_{red} to CAC_{ox} . Furthermore, when the polymer concentration in aqueous solution is above its CAC_{ox} , these polymers can self-assemble into two different aggregates in aqueous solution by redox reaction. For example, wormlike micelles and vesicles can be respectively obtained for the reduction state and oxidation state of polymer 3, while spherical micelles with two different sizes can be obtained for the reduction state and oxidation state of polymer 5. Further, rhodamine 6G (R6G)-loaded polymer aggregates have been successfully used for the oxidation-controlled release of loaded molecules based on their reversible redox-controlled self-assembly behavior, and the release rate of R6G could be mediated by the concentration of both oxidant and copolymers. The results provide an effective approach to the reversible self-assembly of linear-dendritic amphiphilic block copolymer systems without changing their molecular structure and also indicate the potentials of these novel redox-responsive amphiphilic block copolymers in drug delivery systems, catalyst supports, and other research fields.

ASSOCIATED CONTENT

S Supporting Information

Molecular weight, molecular weight distribution, and FT-IR spectra of polymers 3 and 5. ¹H NMR spectrum of polymer 5 recorded in CDCl_3 . Redox reactions of polymer 3. Cyclic voltammograms of polymers 3 and 5 at different scan rates. UV-vis spectra of polymers 3 and 5 before and after oxidation. Absorption intensity of R6G at 527 nm in different concentrations of aqueous solutions. Cumulative release of R6G-loaded 5.0 g L⁻¹ polymer 5 solution after oxidation by different concentrations of oxidant $\text{Fe}_2(\text{SO}_4)_3$. This material is available free of charge via the Internet at <http://pubs.acs.org>.

AUTHOR INFORMATION

Corresponding Author

*Tel/Fax: +86-20-87112708. E-mail: mcbyren@scut.edu.cn.

Notes

The authors declare no competing financial interest.

ACKNOWLEDGMENTS

Financial support from the NSFC (21274047) and the Specialized Research Fund for the Doctoral Program of the Education Ministry (20120172110005) is gratefully acknowledged.

REFERENCES

- (1) Robert, F. How far can we push Chemical Self Assembly? *Science* **2005**, *309*, 95.
- (2) Wang, Y. P.; Xu, H. P.; Zhang, X. Tuning the Amphiphilicity of Building Blocks: Controlled Self-Assembly and Disassembly for Functional Supramolecular Materials. *Adv. Mater.* **2009**, *21*, 2849–2864.
- (3) Wyman, I.; Liu, G. J. Self-assembly and chemical processing of block copolymers: A roadmap towards a diverse array of block copolymer nanostructures. *Sci. China: Chem.* **2013**, *56*, 1040–1066.
- (4) Li, M.-H.; Keller, P. Stimuli-responsive polymer vesicles. *Soft Matter* **2009**, *5*, 927–937.
- (5) Ward, M. D.; Raithby, P. R. Functional behaviour from controlled self-assembly: challenges and prospects. *Chem. Soc. Rev.* **2013**, *42*, 1619–1636.
- (6) Rosen, B. M.; Wilson, C. J.; Wilson, D. A.; Peterca, M.; Imam, M. R.; Percec, V. Dendron-mediated self-assembly, disassembly, and self-organization of complex systems. *Chem. Rev.* **2009**, *109*, 6275–6540.
- (7) MacLeod, J. M.; Rosei, F. Molecular Self-Assembly on Graphene. *Small* **2014**, *10*, 1038–1049.
- (8) Kim, J. K.; Lee, E.; Lee, M. Nanofibers with Tunable Stiffness from Self-Assembly of an Amphiphilic Wedge-Coil Molecule. *Angew. Chem., Int. Ed.* **2006**, *45*, 7195–7198.
- (9) Ott, C.; Hoogenboom, R.; Hoeppener, S.; Wouters, D.; Gohy, J. F.; Schubert, U. S. Tuning the morphologies of amphiphilic metallo-supramolecular triblock terpolymers: from spherical micelles to switchable vesicles. *Soft Matter* **2009**, *5*, 84–91.
- (10) Ren, H. F.; Wu, Y. T.; Ma, N.; Xu, H. P.; Zhang, X. Side-chain selenium-containing amphiphilic block copolymers: redox-controlled self-assembly and disassembly. *Soft Matter* **2012**, *8*, 1460–1466.
- (11) Xiao, Z.-P.; Cai, Z.-H.; Liang, H.; Lu, J. Amphiphilic block copolymers with aldehyde and ferrocene-functionalized hydrophobic block and their redox-responsive micelles. *J. Mater. Chem.* **2010**, *20*, 8375–8381.
- (12) Ma, N.; Li, Y.; Xu, H. P.; Wang, Z. Q.; Zhang, X. Dual redox responsive assemblies formed from diselenide block copolymers. *J. Am. Chem. Soc.* **2010**, *132*, 442–443.
- (13) Xiong, W.; Wang, H. F.; Han, Y. C. Oxidation induced self-assembly transformation of dendron-b-oligoaniline-b-dendron dumbbell shape triblock oligomer. *Soft Matter* **2011**, *7*, 8516–8524.
- (14) Wang, C.; Guo, Y.; Wang, Y.; Xu, H.; Zhang, X. Redox responsive supramolecular amphiphiles based on reversible charge transfer interactions. *Chem. Commun.* **2009**, 5380–5382.
- (15) Napoli, A.; Boerakker, M. J.; Tirelli, N.; Nolte, R. J. M.; Sommerdijk, N. A. J. M.; Hubbell, J. A. Glucose-oxidase Based Self-Destructing Polymeric Vesicles. *Langmuir* **2004**, *20*, 3487–3491.
- (16) Hu, J. M.; Dai, L.; Liu, S. Y. Analyte-reactive amphiphilic thermoresponsive diblock copolymer micelles-based multifunctional ratiometric fluorescent chemosensors. *Macromolecules* **2011**, *44*, 4699–4710.
- (17) Luo, C. H.; Liu, Y.; Li, Z. B. Thermo- and pH-Responsive Polymer Derived from Methacrylamide and Aspartic Acid. *Macromolecules* **2010**, *43*, 8101–8108.
- (18) Ge, Z. S.; Luo, S. Z.; Liu, S. Y. Syntheses and self-assembly of poly (benzyl ether)-b-poly (N-isopropylacrylamide) dendritic-linear diblock copolymers. *J. Polym. Sci., Part A: Polym. Chem.* **2006**, *44*, 1357–1371.
- (19) Chiang, P. R.; Lin, T. Y.; Tsai, H. C.; Chen, H. L.; Liu, S. Y.; Chen, F. R.; Hwang, Y. S.; Chu, I. M. Thermosensitive Hydrogel from Oligopeptide-Containing Amphiphilic Block Copolymer: Effect of Peptide Functional Group on Self-Assembly and Gelation Behavior. *Langmuir* **2013**, *29*, 15981–15991.
- (20) Wang, C.; Chen, Q. S.; Xu, H. P.; Wang, Z. Q.; Zhang, X. Photoresponsive Supramolecular Amphiphiles for Controlled Self-Assembly of Nanofibers and Vesicles. *Adv. Mater.* **2010**, *22*, 2553–2555.
- (21) Rabnawaz, M.; Liu, G. J. Preparation and Application of a Dual Light-Responsive Triblock Terpolymer. *Macromolecules* **2012**, *45*, 5586–5595.
- (22) Njikang, G.; Liu, G. J.; Hong, L. Z. Chiral imprinting of diblock copolymer single-chain particles. *Langmuir* **2011**, *27*, 7176–7184.
- (23) Han, P.; Li, S.; Cao, W.; Li, Y.; Sun, Z. W.; Wang, Z. Q.; Xu, H. P. Red light responsive diselenide-containing block copolymer micelles. *J. Mater. Chem. B* **2013**, *1*, 740–743.
- (24) del Barrio, J.; Oriol, L.; Sánchez, C.; Serrano, J. L.; Di Cicco, A.; Keller, P.; Li, M.-H. Self-Assembly of Linear–Dendritic Diblock Copolymers: From Nanofibers to Polymersomes. *J. Am. Chem. Soc.* **2010**, *132*, 3762–3769.
- (25) Ali, S. I.; Heuts, J. P.; van Herk, A. M. Vesicle-templated pH-responsive polymeric nanocapsules. *Soft Matter* **2011**, *7*, 5382–5390.
- (26) Versluis, F.; Tomatsu, I.; Kehr, S.; Fregonese, C.; Tepper, A. W.; Stuart, M. C.; Ravoo, B. J.; Koning, R. I.; Kros, A. Shape and release control of a peptide decorated vesicle through pH sensitive orthogonal supramolecular interactions. *J. Am. Chem. Soc.* **2009**, *131*, 13186–13187.
- (27) Gillies, E. R.; Jonsson, T. B.; Fréchet, J. M. J. Stimuli-responsive supramolecular assemblies of linear-dendritic copolymers. *J. Am. Chem. Soc.* **2004**, *126*, 11936–11943.
- (28) Yan, Q.; Yuan, J. Y.; Cai, Z. N.; Xin, Y.; Kang, Y.; Yin, Y. W. Voltage-responsive vesicles based on orthogonal assembly of two homopolymers. *J. Am. Chem. Soc.* **2010**, *132*, 9268–9270.
- (29) Yan, Q.; Feng, A.; Zhang, H.; Yin, Y.; Yuan, J. Redox-switchable supramolecular polymers for responsive self-healing nanofibers in water. *Polym. Chem.* **2013**, *4*, 1216–1220.
- (30) Feng, A. C.; Yan, Q.; Zhang, H. J.; Peng, L.; Yuan, J. Y. Electrochemical redox responsive polymeric micelles formed from amphiphilic supramolecular brushes. *Chem. Commun.* **2014**, *50*, 4740–4742.
- (31) Park, C.; Lee, S.; Song, Y.; Rhue, M.; Kim, C. Cyclodextrin-covered organic nanotubes derived from self-assembly of dendrons and their supramolecular transformation. *Proc. Natl. Acad. Sci. U.S.A.* **2006**, *103*, 1199–1203.
- (32) Wang, C.; Chen, Q. H.; Wang, Z. Q.; Zhang, X. An Enzyme-Responsive Polymeric Superamphiphile. *Angew. Chem.* **2010**, *122*, 8794–8797.
- (33) Wang, Y.; Han, P.; Xu, H.; Wang, Z.; Zhang, X.; Kabanov, A. V. Photocontrolled self-assembly and disassembly of block ionomer complex vesicles: A facile approach toward supramolecular polymer nanocontainers. *Langmuir* **2009**, *26*, 709–715.
- (34) Cheng, C. X.; Tian, Y.; Shi, Y. Q.; Tang, R. P.; Xi, F. Ordered Honeycomb-Structured Films from Dendronized PMA-b-PEO Rod-Coil Block Copolymers. *Macromol. Rapid Commun.* **2005**, *26*, 1266–1272.
- (35) Schacher, F. H.; Freier, U.; Steiniger, F. Hierarchical self-assembly of star-shaped organometallic crystalline-coil block copolymers in solution. *Soft Matter* **2012**, *8*, 6968–6978.
- (36) Riess, G. Micellization of block copolymers. *Prog. Polym. Sci.* **2003**, *28*, 1107–1170.
- (37) Dreiss, C. A. Wormlike micelles: where do we stand? Recent developments, linear rheology and scattering techniques. *Soft Matter* **2007**, *3*, 956–970.
- (38) Schacher, F. H.; Rupar, P. A.; Manners, I. Functional block copolymers: nanostructured materials with emerging applications. *Angew. Chem., Int. Ed.* **2012**, *51*, 7898–7921.
- (39) Cai, H. H.; Jiang, G. L.; Chen, C. Y.; Li, Z. B.; Shen, Z. H.; Fant, X. H. New Morphologies and Phase Transitions of Rod-Coil Dendritic-Linear Block Copolymers Depending on Dendron Generation and Preparation Procedure. *Macromolecules* **2014**, *47*, 146–151.
- (40) Abdelkader, H.; Alani, A. W. G.; Alany, R. G. Recent advances in non-ionic surfactant vesicles (niosomes): self-assembly, fabrication,

characterization, drug delivery applications and limitations. *Drug Delivery* **2014**, *21*, 87–100.

(41) Pinedo-Martin, G.; Castro, E.; Martin, L.; Alonso, M.; Rodriguez-Cabello, J. C. Effect of Surfactants on the Self-Assembly of a Model Elastin-like Block Corecombinamer: From Micelles to an Aqueous Two-Phase System. *Langmuir* **2014**, *30*, 3432–3440.

(42) Bajpai, A.; Shukla, S. K.; Bhanu, S.; Kankane, S. Responsive polymers in controlled drug delivery. *Prog. Polym. Sci.* **2008**, *33*, 1088–1118.

(43) Blasco, E.; Serrano, J. L.; Piñol, M.; Oriol, L. Light Responsive Vesicles Based on Linear–Dendritic Block Copolymers Using Azobenzene–Aliphatic Codendrons. *Macromolecules* **2013**, *46*, 5951–5960.

(44) Napoli, A.; Boerakker, M. J.; Tirelli, N.; Nolte, R. J.; Sommerdijk, N. A.; Hubbell, J. A. Glucose-oxidase based self-destructing polymeric vesicles. *Langmuir* **2004**, *20*, 3487–3491.

(45) Wang, Z. P.; Möhwald, H.; Gao, C. Y. Preparation and Redox-Controlled Reversible Response of Ferrocene-Modified Poly (allylamine hydrochloride) Microcapsules. *Langmuir* **2010**, *27*, 1286–1291.

(46) Eloi, J.-C.; Rider, D. A.; Cambridge, G.; Whittell, G. R.; Winnik, M. A.; Manners, I. Stimulus-responsive self-assembly: reversible, redox-controlled micellization of polyferrocenylsilane diblock copolymers. *J. Am. Chem. Soc.* **2011**, *133*, 8903–8913.

(47) Rider, D. A.; Winnik, M. A.; Manners, I. Redox-controlled micellization of organometallic block copolymers. *Chem. Commun.* **2007**, 4483–4485.

(48) van Staveren, D. R.; Metzler-Nolte, N. Bioorganometallic chemistry of ferrocene. *Chem. Rev.* **2004**, *104*, 5931–5985.

(49) Aydogan, N.; Gallardo, B. S.; Abbott, N. L. A molecular-thermodynamic model for Gibbs monolayers formed from redox-active surfactants at the surfaces of aqueous solutions: redox-induced changes in surface tension. *Langmuir* **1999**, *15*, 722–730.

(50) Chandar, P.; Somasundaran, P.; Turro, N. J. Fluorescence probe investigation of anionic polymer-cationic surfactant interactions. *Macromolecules* **1988**, *21*, 950–953.

(51) Li, C. Q.; Ren, B. Y.; Zhang, Y.; Cheng, Z. Y.; Liu, X. X.; Tong, Z. A Novel Ferroceneylazobenzene Self-Assembled Monolayer on an ITO Electrode: Photochemical and Electrochemical Behaviors. *Langmuir* **2008**, *24*, 12911–12918.

(52) Ding, J. F.; Liu, G. J. Growth and Morphology Change of Polystyrene-b lock-poly (2-cinnamoylethyl methacrylate) Particles in Solvent-Nonsolvent Mixtures before Precipitation. *Macromolecules* **1999**, *32*, 8413–8420.

(53) Cheng, Z. Y.; Ren, B. Y.; Liu, R.; Chang, X. Y.; Tong, Z. Synthesis and characterization of novel redox-active percec-type dendrons. *Chin. Chem. Lett.* **2012**, *23*, 438–441.

(54) Zhou, Z. X.; Ma, X. P.; Jin, E. L.; Tang, J. B.; Sui, M. H.; Shen, Y. Q.; Van Kirk, E. A.; Murdoch, W. J.; Radosz, M. Linear-dendritic drug conjugates forming long-circulating nanorods for cancer-drug delivery. *Biomaterials* **2013**, *34*, 5722–5735.

(55) Antonietti, M.; Förster, S. Vesicles and Liposomes: A Self-Assembly Principle Beyond Lipids. *Adv. Mater.* **2003**, *15*, 1323–1333.

(56) van Hest, J. C. M.; Delnoye, D. A. P.; Baars, M. W. P. L.; van Genderen, M. H. P.; Meijer, E. W. Polystyrene-Dendrimer Amphiphilic Block Copolymers with a Generation-Dependent Aggregation. *Science* **1995**, *268*, 1592–1595.